

# Exploratory Adaptation in Large Random Networks

Hallel I. Schreier<sup>1,2</sup>, Yoav Soen<sup>3</sup>, and Naama Brenner<sup>1,4,\*</sup>

<sup>1</sup>Network Biology Research Laboratories, Technion - Israel Institute of Technology, Haifa 32000, Israel

<sup>2</sup>Interdisciplinary Program of Applied Mathematics, Technion - Israel Institute of Technology, Haifa 32000, Israel

<sup>3</sup>Department of Biological Chemistry, Weizmann Institute of Science, Rehovot 76100, Israel

<sup>4</sup>Department of Chemical Engineering, Technion - Israel Institute of Technology, Haifa 32000, Israel

\*Corresponding Author: nbrenner@tx.technion.ac.il

**The capacity of cells and organisms to respond in a repeatable manner to challenging conditions is limited by a finite number of pre-evolved adaptive responses. Beyond this capacity, exploratory dynamics can provide alternative means to cope with a much broader array of conditions [1, 2, 3]. At the population level, exploration is implemented by mutations and selection over multiple generations. However, within the lifetime of a single cell, the mechanisms by which exploratory changes can lead to adaptive phenotypes are still poorly understood. Here, we address this question by developing a network model of exploration in gene regulation. The model we propose demonstrates the feasibility of adapting by temporal exploration. Exploration is initiated by failure to comply with a global constraint and is implemented by random sampling of available network configurations. It ceases if and when the system converges to a stable compliance with the constraint. Successful convergence of this process depends crucially on network topology and is most efficient for scale-free connectivity, typical of gene regulatory networks. For such networks, convergence to an adapted phenotype can be achieved without fine tuning of initial conditions or other model parameters, thus making it plausible for biological implementation.**

The ability to organize a large number of interacting processes into persistently viable states in a dynamic environment is a striking property of cells and organisms. Many frequently encountered perturbations (temperature, osmotic pressure, starvation and more), trigger reproducible adaptive responses [4, 5, 6]. These were assimilated into the system by variation and selection over evolutionary time. Despite the large number and flexible nature of these responses, they span a finite repertoire of actions and cannot address all possible scenarios of novel conditions. Indeed, cells may encounter severe, unforeseen situations within their lifetime, for which no effective response is available. To survive

such challenges, a different type of ad-hoc response can be employed, utilizing exploratory dynamics [2, 3].

The capacity to withstand unforeseen conditions was recently demonstrated and studied using dedicated experimental models of novel challenge in yeast [7, 8, 9] and flies [10]. Adaptive responses exposed in these experiments involved transient changes in the expression of hundreds of genes, followed by convergence to altered patterns of expression. Analysis of repeated experiments showed that a large fraction of the transactional response can vary substantially across replicate trajectories of adaptation [7]. These findings suggest that coping

with unforeseen challenges within one or a few generations relies on induction of exploratory changes in gene regulation along time [1, 2, 3].

Several properties of gene regulatory networks may support such exploratory adaptation. These include a large number of potential interactions between genes [11], context-dependent plasticity of interactions [12, 13, 14] and multiplicity of microscopic configurations consistent with a given phenotype [15]. Despite these properties, the feasibility of generating new adaptive phenotype by exploratory changes in time remains speculative and poorly understood. In particular, it is not known how exploration may converge rapidly enough in the high dimensional space of possible configurations? what determines the efficiency of this exploration? and what organizing principle may underlie stabilization of new phenotypes?

To investigate the feasibility of adaptation by exploratory dynamics, we introduce a network model inspired by properties of gene regulation. The model consists of a large number,  $N$ , of microscopic components  $\vec{x} = (x_1, x_2 \dots x_N)$ , governed by the following nonlinear equation of motion (Fig. 1A):

$$\dot{\vec{x}} = W\phi(\vec{x}) - \vec{x}, \quad (1)$$

where  $W$  is a random interaction matrix,  $\phi(\vec{x})$  a saturating function restricting the variables' dynamic range and the relaxation rates are normalized to unity. This equation describes complex regulatory interactions of gene products, representing intracellular dynamics. Previous work has used similar equations to address evolutionary aspects of gene regulation [16, 17], as well as interactions and relaxation in neuronal networks [18]. This body of work has focused primarily on networks with uniform (full or sparse) connectivity. Little is known, however, about these dynamics for networks with non-uniform topological structures, which may be of relevance to gene regulation.

Here we consider sparse random matrices with properties inspired by empirical evidence in gene

regulatory networks. The interaction matrix  $W$  is composed of an element-wise (Hadamard) product,

$$W = T \circ J, \quad (2)$$

where  $T$  is a topological backbone (adjacency) matrix with binary (0/1) entries representing potential interaction between the network elements; and  $J$  is a random matrix specifying the actual interaction strengths. We will emphasize below network sizes and topological structures that are relevant to gene regulatory networks. To represent context-dependent plasticity, we assume that the backbone remains fixed, whereas the interaction strengths are plastic and amenable to change over time.

On a macroscopic level, the cell exhibits a phenotype,  $y$ , which depends on many microscopic components and determines the cell's functionality. We define this phenotype as a linear combination

$$y(t) = \vec{b} \cdot \vec{x}(t) \quad (3)$$

with an arbitrary vector of coefficients  $\vec{b}$ . Any value of the phenotype can therefore be realized by a large number of alternative microscopic combinations. To model an unforeseen challenge, this phenotype is subjected to an arbitrary constraint  $y(\vec{x}(t)) \approx y^*$ .

Deviation from compliance with the constraint is mediated by a global cellular variable  $\mathcal{M}(y - y^*)$ , representing the level of mismatch between the current phenotype and the demand. This mismatch is effectively zero inside a "comfort zone" of size  $\varepsilon$  around  $y^*$  and increases sharply beyond this zone. Importantly, this implies that the constraint is satisfied in a region around  $y^*$ , in contrast to optimization problems which require adherence to a specific value.

When the phenotype deviates from the comfort zone, the mismatch drives an exploratory search. The plasticity of regulatory interactions can now be utilized to sample different network configurations. This is realized by making small changes in the interaction strengths, amounting to a random walk in

the elements of the matrix  $J$ :

$$\begin{aligned} dJ_t &= \sqrt{D \cdot \mathcal{M}(y - y^*)} \cdot d\mathcal{W}_t, \\ J(t=0) &= J_0, \end{aligned} \quad (4)$$

where  $\mathcal{W}_t$  is the standard Wiener process and the amplitude of the random walk is controlled by the a scale parameter  $D$  and the mismatch level  $\mathcal{M}$ . This random walk constitutes an exploratory search for a network configuration in which the dynamical system (Eq. (1)) can satisfy the constraint in a stable manner. Random occurrence of such a configuration decreases the search amplitude, thereby promoting its relaxation by reducing the drive for exploration. [3, 19].

Convergence to a stable state satisfying the constraint is not *a-priori* guaranteed. Intuitively, it may be expected that randomly varying a large number of parameters in a nonlinear high-dimensional system, will cause the dynamics to diverge. Surprisingly, we find the adaptation processes described above can in fact converge; however, convergence is not universal and depends strongly on network properties. Networks with a scale-free topological backbone are much more likely to converge.

An example of adaptive dynamics in such a network is shown in Fig. 1B-D. At  $t = 0$ , the system is confronted with a demand and starts an exploratory process in which the connection strengths are slowly modified. Fig. 1B displays four connection strengths over time. During this exploration the microscopic components  $\vec{x}$  and the phenotype  $y$  exhibit highly irregular trajectories, rapidly sampling a large dynamic range (Fig. 1C, 1D respectively). At  $t = 400$ , the system manages to stably reduce the mismatch to zero and to converge to a fixed point within the comfort zone  $\pm \varepsilon$  around  $y^*$  (see supplementary data for an example of convergence to a small-amplitude limit-cycle). The difference between the trajectories in Fig. 1 B and those in Fig. 1 C-D reflects the separation of timescales between the intrinsic dynamics of Eq. (1) and the slowly accumulating change of

interaction strengths, governed by Eq. (3). Notably, convergence is achieved before the accumulation of large changes in the connection strengths.

As mentioned above, convergence depends crucially on the topological structure of the network. To examine this dependence, we construct random matrix ensembles with different topological backbones, and compute for each the fraction of simulations which converged within a given time window. Fig. 2A compares ensembles of networks with in- and out-degrees drawn from Binomial, Exponential (Exp) and Scale-Free (SF) distributions. It shows high fractions of convergence, 0.5 or higher, only for ensembles with SF out-degree distributions. In contrast, the in-degree distribution affects convergence only mildly. For example, the convergence fraction of networks with SF out-degree and Binomial in-degree distributions (dark blue) is 0.5, as opposed to 0.03 in the opposite case (light blue).

Remarkably, gene regulatory networks exhibit SF out-degree and Exponential in-degree distributions [20, 21], corresponding to an ensemble with highly efficient exploratory adaptation. Specifically, genes with high out-degrees are substantially more abundant than genes with high in-degree. Examples of genes with high out-degree are transcription factors which can regulate hundreds of other genes.

Analysis of convergence fractions as a function of network size shows that the effect of topology becomes pronounced for large networks (Fig. 2B). Convergence in small to intermediate-sized networks ( $N \lesssim 200$ ) is higher and relatively independent of topology. However, as  $N$  increases towards sizes that are typical of genetic networks, the benefit of having SF out-degree distribution becomes progressively prominent.

In addition to network topology, interactions within the network are determined by the connections strength,  $J_{ij}$ . These strengths are initially drawn from a Gaussian distribution with a zero mean and a given standard deviation. The normalized standard deviation,  $g_0$  (also called network

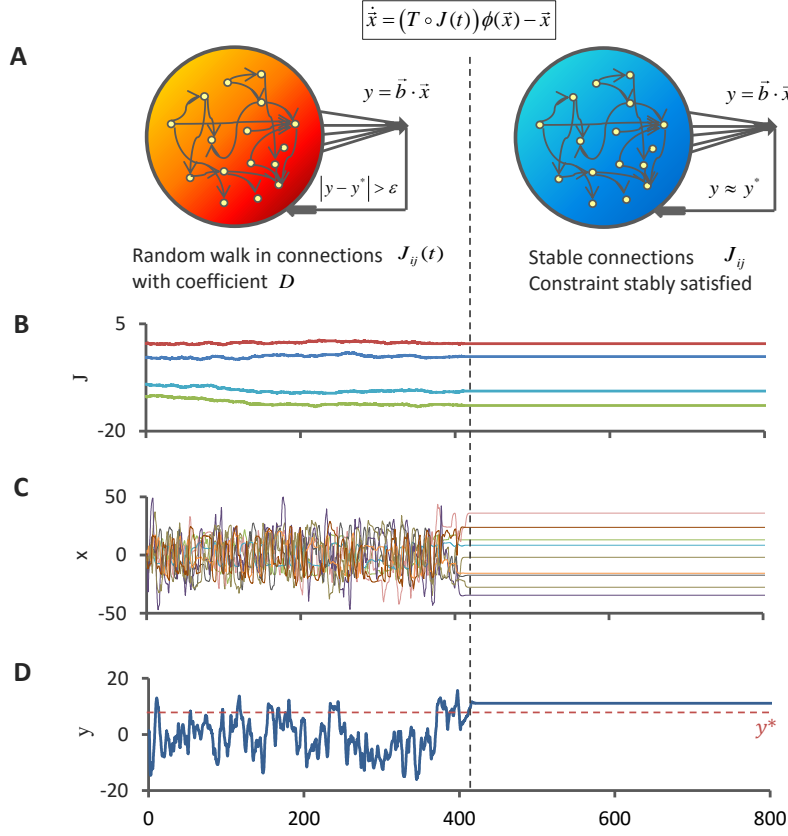


**Figure 1: Exploratory dynamics and convergence to a stable state.** (A). Schematic representation of the model: a random  $N \times N$  network, described by an adjacency matrix  $T$  and an interaction strength matrix  $J$ , defines a nonlinear dynamical system (equation in box). The resulting spontaneous dynamics are typically irregular for large enough interactions. A macroscopic variable, the phenotype  $y$ , is subject to an arbitrary constraint  $y \approx y^*$  with finite precision  $\varepsilon$ . Following a mismatch with respect to this constraint, the connections strengths  $J_{ij}$  undergo an exploratory random walk with coefficient  $D$  (left; "hot" regime), which stops when a stable mismatch-decreasing configuration is encountered (right; "frozen" regime). (B) Sample trajectories of connection strengths, elements of the matrix  $J$ , during exploratory dynamics and following stabilization. (C) Sample trajectories of  $\vec{x}$ -components showing irregular dynamics and convergence to a fixed point satisfying the constraint. (D) Trajectory of the phenotype  $y$  and its convergence to a value stably satisfying the external constraint,  $y \approx y^*$ . Note that the constraint is satisfied several times before convergence as the trajectory passes through  $y^*$ . The network has scale-free (SF) out-degree distribution with  $a=1$ ,  $\gamma=2.4$  and Binomial in-degree distribution with  $p \simeq \frac{3.5}{N}$  and  $N$ .  $N=1000$ ,  $y^*=10$ ,  $D=10^{-3}$ , and initial gain  $g_0=10$ .

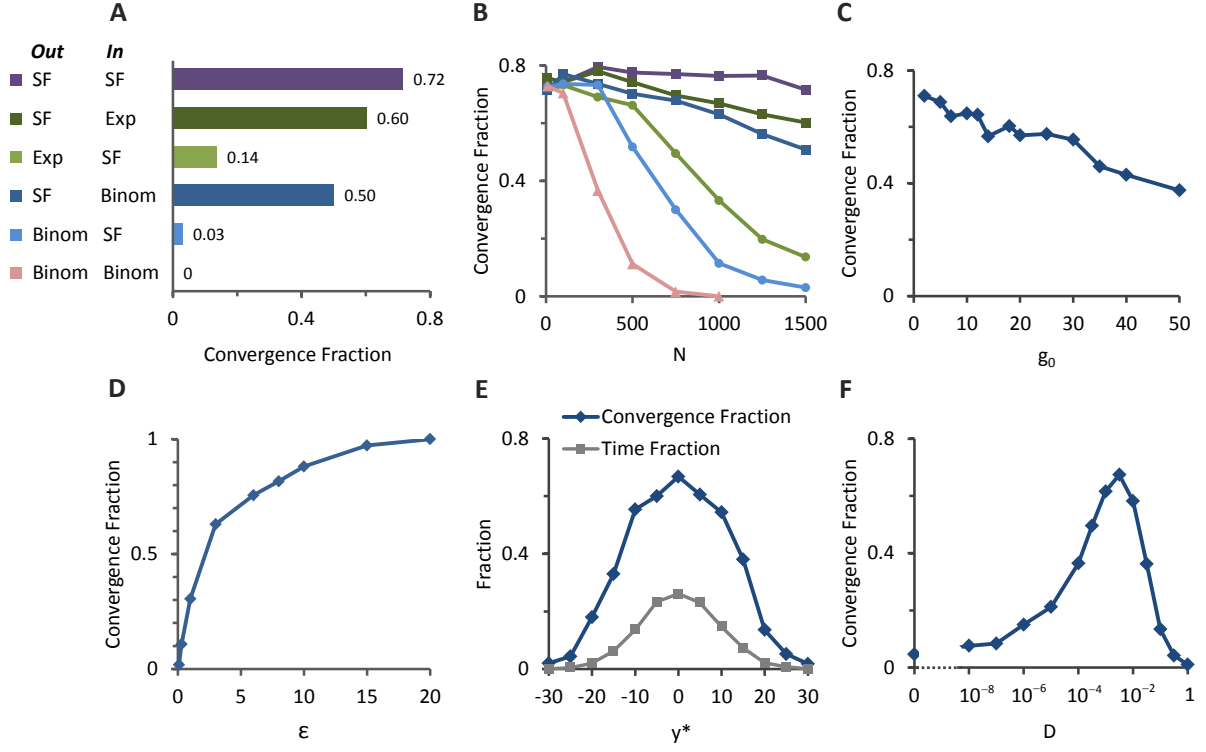


**Figure 2: Convergence Fractions (CF) in a fixed time window.** (A) Seven ensembles of networks of size  $N=1500$  and different topologies display remarkably different convergence fractions. Ensembles are characterized by the out and in degree distributions of the backbone adjacency matrix  $T$ : 'SF', scale free distribution; 'Exp', exponential distribution; 'Binom', Binomial distribution. Interaction strengths at nonzero entries of this backbone are drawn independently from a Gaussian distribution (see Methods for details). For fully or sparsely connected homogeneous random networks the CF is close to zero. (B) CF as a function of network size for the same ensembles of (A) with matching colors. C-F present results for the SF(out)-Binom(in) ensemble. (C) CF vs. initial network gain (proportional to the std of connection strengths). (D) CF vs.  $\epsilon$ , width of comfort zone around  $y^*$ . (E) CF vs. value of constraint  $y^*$  (blue). For comparison, the fraction of time  $y$  spontaneously encountered the required range of phenotype over a long trajectory prior to convergence is shown (grey). (F) CF vs.  $D$ , the effective diffusion coefficient for exploratory random walk in connection strengths. All CF were computed within 2000 time steps in ensembles of 500 networks with random  $T$ ,  $J_0$  and  $\vec{x}_0$ . Unless otherwise mentioned, all ensembles have  $N = 1000$ ,  $y^* = 0$ ,  $g_0 = 10$ , and  $D = 10^{-3}$ . Parameters for degree distributions: SF,  $a = 1$ ,  $\gamma = 2.4$ ; Binom,  $(p \simeq \frac{3.5}{N}, N)$ ; Exp,  $\beta \simeq 3.5$ .

gain) determines the contribution of the first vs. second term in eq (1). In large homogeneous networks, this parameter determines whether the dynamics is dissipative ( $g_0 < 1$ ) or chaotic ( $g_0 > 1$ ) [22]. It is not known, however, how this parameter affects the dynamics of SF networks. Fig. 2C shows the convergence fraction as a function of  $g_0$ , for an ensemble with a SF-Binom backbone, showing a rather weak decrease with this parameter.

Figs. 2D-E show how the convergence fraction depends on the severity of the constraint. Fig. 2D examines the effect of increasing severity by reducing the size of the comfort zone  $\varepsilon$ , revealing a sharp decrease of the convergence fraction at small  $\varepsilon$ . This shows that a non-vanishing comfort zone is crucial for successful exploratory adaptation. This property of the constraint is biologically plausible, as one expects a range of phenotypes to be fit to a given environment rather than a narrowly defined exactly optimal one. Another way of increasing severity is by shifting the range of required phenotype away from the origin. Reaching a shifted range is more challenging since these regions are rarely visited by the spontaneous dynamics (Fig. 2E, gray curve). Indeed, the blue curve in Fig. 2E shows that the convergence fraction decreases as  $y^*$  moves away from zero. However, it always remains much larger than the probability of encountering the required phenotype spontaneously. For example, a non-negligible fraction of convergence (0.2) is observed even for  $|y^*| \sim 20$  that is spontaneously encountered with probability of 0.02.

To evaluate the sensitivity of adaptation to exploration speed, we varied the effective diffusion coefficient in the space of connection-strengths,  $D$ . Fig. 2F shows that a nonzero convergence fraction is achieved for a wide range of this parameter and remains between 0.2–0.7 over more than 5 decades of  $D$ . As the value of  $D$  increases above a certain level, where the separation of timescales ceases to hold, the convergence fraction decreases drastically.

The results of Fig. 2 show that outgoing SF de-

gree distribution is a prominent feature of network ensembles facilitating convergence. We therefore evaluate more closely the contribution of outgoing hubs (most highly connected nodes) in such ensembles. Fig. 3A shows the influence on convergence fractions of deleting outgoing hubs vs. deleting random nodes [23]. It reveals that the ability to converge by exploratory dynamics is strongly and primarily affected by a small number of outgoing hubs. Furthermore, comparison between SF network ensembles with different degrees of the leading hub, displays a positive correlation between hub degree and convergence fraction (Fig. 3B). These results indicate that outgoing hubs have a major organizing role in the convergence process.

So far, our analysis focused on the convergence fractions within a fixed time interval. To characterize the temporal aspects of the exploratory adaptation process, we evaluate the convergence-time distribution in repeated long simulations. Fig. 4 reveals a broad distribution ( $CV \approx 1.1$ ), well fitted by a stretched exponential (see also Supp. Fig. S8). Such distributions are common in complex systems [24] and were suggested to reflect a hierarchy of timescales [25]. Similarly shaped distributions were found in all topological ensembles tested; however, networks with SF out-degree distribution typically converge faster than their opposite ensembles (Fig. 4A). Moreover, deletion of a small number of leading outgoing hubs causes a significant shift towards slower convergence times (Fig. 4B). Thus, networks with larger heterogeneity in out-degrees are more likely to converge within a set time window (Figs. 2A, 3A), and typically converge faster (Fig. 4).

The intrinsic nonlinear dynamics of Eq. (1), with a strongly heterogeneous network structure, is largely uninvestigated. To evaluate the effect of network topology on the intrinsic dynamics of such a system, we estimated fractions of convergence to fixed points in fixed networks. This measure is analogous to the convergence fraction used in Fig. 2, but without a constraint or random walk in connection strengths. Results show that the ability of a

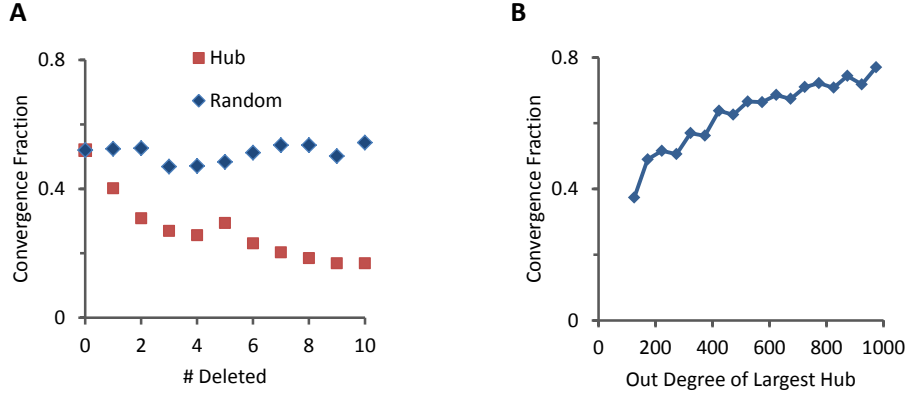


Figure 3: **Convergence fraction dependence on network hubs.** (A) Effect of deliberately deleting the leading hubs (red) vs deleting random nodes (blue) on convergence fraction in a SF-out Binom-in network ensemble. 500 networks were simulated over 2000 time steps for each point. (B) Convergence fraction vs. out-degree of leading hub. CF were binned according to largest hub from a large set of simulations with  $T$  drawn from SF-out Binom-in degree distributions.  $N = 1500$ ,  $y^* = 0$ ,  $g_0 = 10$ , and  $D = 10^{-3}$ . Parameters for degree distributions: SF, ( $a = 1$ ,  $\gamma = 2.4$ ); Binom, ( $p \simeq \frac{3.5}{N}$ ,  $N$ ).

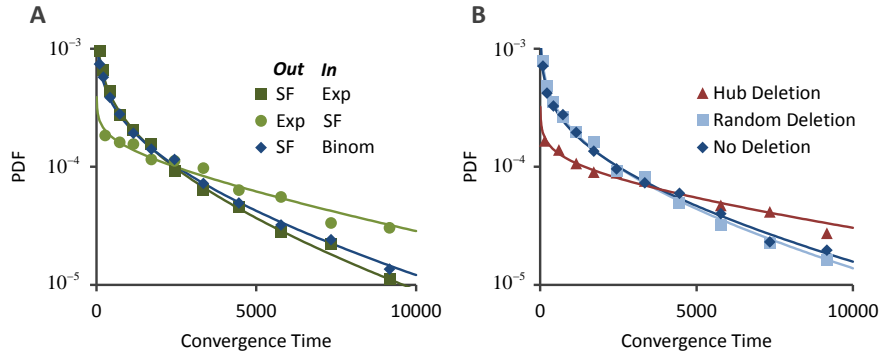
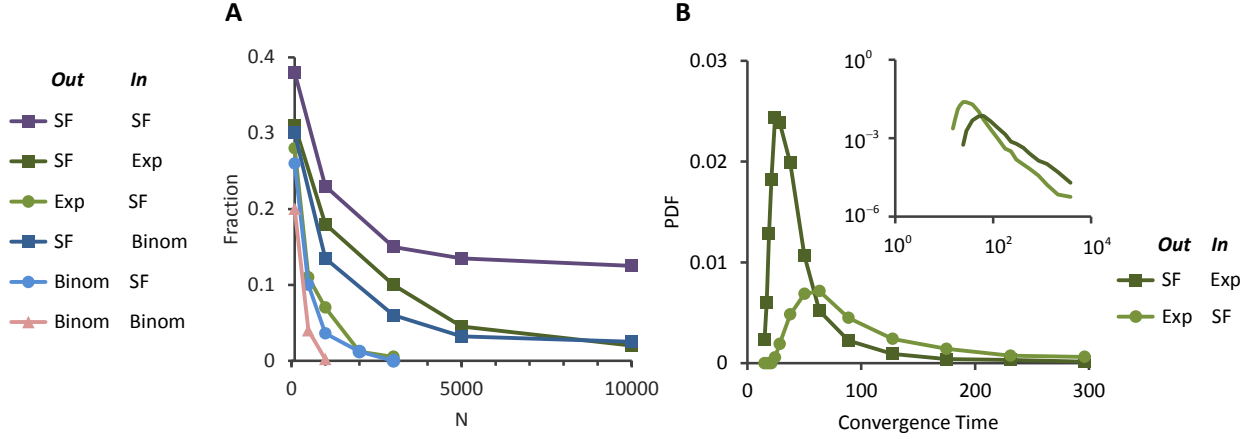


Figure 4: **Distribution of convergence times.** For those networks which converged in less than  $10^4$  timesteps, the probability distribution (PDF) of time to convergence is plotted. All distributions shown decay extremely slowly (solid lines: stretched exponential fits). (A) Convergence time distribution for three topological ensembles. (B) The effect of random node deletion (light blue) and deletion of 8 maximal hubs (red) on the distribution, for the SF(out)-Binom(in) ensemble. Ensembles in both panels consist of networks with random  $T$ ,  $J_0$  and  $\vec{x}_0$ . All ensembles have  $N = 1000$ ,  $y^* = 0$ ,  $g_0 = 10$ , and  $D = 10^{-3}$ . Degree distribution parameters: SF,  $a = 1$ ,  $\gamma = 2.4$ ; Binom, ( $p \simeq \frac{3.5}{N}$ ,  $N$ ); Exp,  $\beta \simeq 3.5$ .



**Figure 5: Intrinsic nonlinear dynamics for different topological ensembles.** (A) Fraction of networks within an ensemble which converged to a fixed point under the nonlinear dynamics of Eq. (1), with a fixed interaction matrix. Compare with Fig. 2B: ensembles which were more successful in exploratory adaptation are those that converged to fixed points with higher probability. (B) Distribution of relaxation times to fixed points for two of the ensembles. Both show broad power-law like tails, but the typical timescale for convergence shorter for the SF-out ensemble (the more successfully adapting ensemble). In both panels  $N = 1000$ ,  $g = 10$ . Degree distribution parameters: SF,  $a = 1$ ,  $\gamma = 2.4$ ; Binom,  $(p \simeq \frac{3.5}{N}, N)$ ; Exp,  $\beta \simeq 3.5$ .

given network to support convergence to a fixed point is largely insensitive to the initial conditions in  $x$ -space (not shown). With that in mind, we computed, for each topological ensemble, the fraction of networks supporting convergence within a fixed time window, starting with random initial conditions. Fig. 5A reveals topology-dependent differences that are qualitatively in line with the results of the exploratory adaption shown above (Fig. 2B). This suggests that a substantial contribution to successful convergence is provided by high abundance of networks exhibiting fixed points in their dynamics.

For each network ensemble exhibiting fixed points in its dynamics, there are also timescales associated with relaxation to these fixed points. Analysis of the distribution of these relaxation times shows that these too are influenced by topology. Fig. 5B demonstrates this by comparing networks with SF-out/Exp-in degrees to the opposite case of Exp-out/SF-in degrees. It shows that networks with SF-out degrees typically support faster relaxation towards their respective fixed points. It may

be expected that faster relaxation to a fixed point would support adaption. This may allow the system to converge to a solution before the random walk has had a chance to significantly modify network connections. Further work is required to broaden the theoretical understanding of these dynamics in random ensembles with heterogeneous topology.

Overall, we have introduced a model of exploratory adaptation driven by mismatch between an internal global variable and an external constraint. The exploration involves a purely random search in the high dimensional space of network connection strengths. We showed that such convergence depends crucially on having a broad distribution of outgoing degrees in the network, while the heterogeneity of incoming degrees is far less important for adaptation. Convergence of exploratory adaptation appears to be a complex process characterized by an extremely broad distribution of times. It likely depends on a delicate interplay between the phase space structure of the different network ensembles, their connectivity properties in the space of networks [17] and the typical timescales of their



intrinsic dynamics.

Our model draws from neural network models [26, 27, 28], but is substantially different in relying on purely stochastic exploratory dynamics. In the language of learning theory, the "task" is modest: convergence to a fixed point (or a small-amplitude trajectory) which satisfies a low-dimensional approximate constraint. Without dynamics, this task could be fulfilled by chance with a very small probability. This probability increases dramatically using exploratory dynamics within an ensemble of networks capable of supporting convergence. The ability to achieve high success rates without a need for complex computation or fine-tuning, makes this type of adaptation particularly plausible for biological implementation.

Previous theoretical work has used random-network models to address evolutionary dynamics of gene regulation over many generations. In this approach, a population of networks undergoes mutations and reproduces according to an assigned fitness [17, 29]. While this line of research differs in timescales, level of organization and biological phenomena from the one presented here, common themes naturally arise with regard to network properties and dynamics [30]. For example, marked differences in evolutionary dynamics were found between homogeneous and SF networks [31]. More generally, gene regulatory networks display multifaceted behavior depending on the type of environment they encounter and the timescales of observation. Thus, the collection of reproducible and exploratory responses in single cells, and the evolutionary processes at the population-level, reflect distinct aspects of gene-environment interactions [6]. These could potentially be integrated into a more general picture where the overall response depends on the type of challenge and spans a broad range of timescales [32].

## Methods

**Network construction.** Networks were constructed using the method described in [1]. Scale-free (SF) random

sequences were sampled by discretization of the Pareto Distribution  $P(k) = \frac{(\gamma - 1)a^{\gamma-1}}{k^\gamma}$ . Sampling SF degree sequences using the discrete Zeta distribution gives qualitatively similar results (results not shown). Exponential degree distributions were sampled by discretization of the Exponential distribution  $P(k) = \frac{1}{\beta}e^{-k/\beta}$ . Initial values of  $J$  are normally distributed with  $J_{0ij} \sim \mathcal{N}(0, \frac{g_0^2}{\langle k \rangle})$ , where  $\langle k \rangle$  is the mean in and out degree of the network and  $g_0$  controls the initial spectral radius of  $W$  (see Supplementary sections 1.1 and 1.2 for details)

**Macroscopic phenotype  $y$**  is defined as  $y(\vec{x}) = \vec{b} \cdot \vec{x}$ . The weight vector  $\vec{b}$  is characterized by a sparseness  $\frac{1}{N} < c < 1$ . Non-zero weights of  $\vec{b}$  are normally distributed with  $b_i \sim \mathcal{N}(0, \frac{1}{g_0^2 \cdot cN} \cdot \alpha)$ , where  $\frac{1}{g_0^2 \cdot cN}$  is a normalizing factor and  $\alpha$  is a scaling parameter controlling the weight variance. For all results shown  $\alpha = 100$  and  $c = 0.2$  (see Supplementary sections 1.3 and 2.3 for details and dependence of convergence on  $c$ ).

**Mismatch function  $\mathcal{M}(y)$**  is defined as a symmetric sigmoid  $\mathcal{M}(y) = \frac{\mathcal{M}_0}{2} (1 - \tanh(\frac{|y| - \varepsilon}{\mu}))$ , where  $\varepsilon$  controls the size of the low-mismatch "comfort-zone" around  $y^*$ ,  $\mu$  controls the steepness of the sigmoid, and  $\mathcal{M}_0$  is its maximal value. A different mismatch function which is zero in the region  $(-\varepsilon, \varepsilon)$  and linear in  $|y|$  outside of this region was also examined and gives qualitatively similar results. Convergence and stability requires a flat region with zero or very low mismatch around  $y^*$ . For all results shown  $\varepsilon = 3$ ,  $\mu = 0.01$  and  $\mathcal{M}_0 = 2$  (see Supplementary section 1.4 for details).

## References

- [1] J. Gerhart and M. Kirschner, "Cells, embryos, and evolution: Toward a cellular and developmental understanding of phenotypic variation and evolutionary adaptability". Malden: Blackwell Science, (1997).
- [2] E. Braun, "The unforeseen challenge: from genotype-to-phenotype in cell populations". Rep. Prog. Phys. **78**, 036602 (2015).
- [3] Y. Soen, M. Knafo and M. Elgart, "A principle of organization which facilitates broad Lamarckian-like adaptations by improvisation". Biology Direct **10**, 68 (2015).
- [4] A.P. Gasch P.T. Spellman C.M. Kao, O. Carmel-Harel M.B. Eisen G. Storz, D. Botstein and P.O. Brown, "Genomic ex-

- pression programs in the response of yeast cells to environmental changes". *Mol Biol Cell*, **11**42414257 (2000).
- [5] H.C. Causton, et al. "Remodeling of Yeast Genome Expression in Response to Environmental Changes". *Mol. Biol. Cell*, 323-33712 (2001).
- [6] L. Lpez-Maury, S. Marguerat and J. Bhler, "Tuning gene expression to changing environments: from rapid responses to evolutionary adaptation". *Nat. Rev. Genet.* **9**, 583-93 (2008).
- [7] S. Stern, T. Dror, E. Stolovicki, N. Brenner and E. Braun, "Genome-wide transcriptional plasticity underlies cellular adaptation to novel challenge", *Mol. Sys. Biol.* **3**, article 106 (2007).
- [8] L. David, E. Stolovicki, E. Haziz and E. Braun, "Inherited adaptation of genome-rewired cells in response to a challenging environment." *HFSP journal* **4**, 131-141 (2010).
- [9] Y. Katzir, E. Stolovicki, S. Shay and E. Braun. "Cellular plasticity enables adaptation to unforeseen cell-cycle rewiring challenges." *PloS one* **7**, e45184 (2012).
- [10] S. Stern, Y. Fridmann-Sirkis, E. Braun and Y. Soen. "Epigenetically heritable alteration of fly development in response to toxic challenge." *Cell reports* **1**, no. 5 (2012): 528-542.
- [11] A.H.Y. Tong, G. Lesage, G. D. Bader, H. Ding, H. Xu, X. Xin, J. Young et al. "Global mapping of the yeast genetic interaction network." *Science* **303**, 808-813 (2004).
- [12] C.T. Harbison et al., "Transcriptional regulatory code of a eukaryotic genome" *Nature* **431**, 99(2004).
- [13] N.M. Luscombe, et al. "Genomic analysis of regulatory network dynamics reveals large topological changes." *Nature* **431** 308-312 (2004).
- [14] K.J. Niklas, S.E. Bondos, A.K. Dunker and S. A. Newman, "Rethinking gene regulatory networks in light of alternative splicing, intrinsically disordered protein domains, and post-translational modifications". *Front. Cell Dev. Biol.* **3**, (2015).
- [15] K. M. Weiss and S. M. Fullerton, "Phenogenetic drift and the evolution of genotype-phenotype relationships". *Theoret. Pop. Biol.* **31**, 187-95 (2000).
- [16] S.A. Kauffman, "Origins of Order: Self-Organization and Selection in Evolution", Oxford University Press (1993).
- [17] A. Wagner, "The Origins of Evolutionary Innovations: A Theory of Transformative Change in Living Systems", Oxford University Press (2011).
- [18] D. J. Amit, "Modeling brain function: The world of attractor neural networks". Cambridge University Press; (1992).
- [19] G. Shahaf and S. Marom, "Learning in networks of cortical neurons." *J. Neurosc.* **21**, 8782-8788 (2001).
- [20] N. Guelzim, S. Bottani, P. Bourguine and F. Kps, "Topological and causal structure of the yeast transcriptional regulatory network", *Nat. Genet.* **31**, 60 (2002).
- [21] S. A. Teichmann and M. M. Babu, "Gene regulatory network growth by duplication." *Nature genetics* **36**, 492-496 (2004).
- [22] H. Sompolinsky, A. Crisanti and H.J. Sommers, "Chaos in Random Neural Networks", *Phys. Rev. Lett.* **61**, 259-262 (1988).
- [23] R. Albert, H. Jeong and A.L. Barabasi, "Error and attack tolerance of complex networks". *Nature*, **406**, 378-82 (2000).
- [24] J. Laherrere and D. Sornette, "Stretched exponential distributions in nature and economy: 'fat tails' with characteristic scales". *Eur. Phys. J. B*, **2**, 525-39 (1998)
- [25] R.G. Palmer, D.L. Stein, E. Abrahams and P.W. Anderson, "Models of Hierarchically Constrained Dynamics for Glassy Relaxation". *Phys. Rev. Lett.* **53**, 958 (1984).
- [26] W. Maass, T. Natschlger and H. Markram, "Real-time computing without stable states: A new framework for neural computation based on perturbations." *Neural computation* **14**, 2531-2560 (2002).
- [27] D. Sussillo and L.F. Abbott. "Generating coherent patterns of activity from chaotic neural networks." *Neuron* **63**, 544-557 (2009).
- [28] O. Barak, et al. "From fixed points to chaos: three models of delayed discrimination." *Prog. Neurobiol.* **103**, 214-222 (2013).
- [29] A. Bergman and M. L. Siegal, "Evolutionary capacitance as a general feature of complex gene networks." *Nature* **424**, 549-552 (2003).
- [30] B. Barzel and A.L. Barabasi, "Universality in network dynamics". *Nature Physics* **9**, 673 (2013).
- [31] P. Oikonomou and P. Cluzel, "Effects of topology on network evolution." *Nature Physics* **2**, 532-536 (2006).
- [32] A.H. Yona, I. Frumkin and Y. Pilpel, "A relay race on the evolutionary adaptation spectrum", *Cell* **163**, 549 (2015).
- [33] H. Kim, C.I. del Genio, K.E. Bassler and Z. Toroczkai, "Constructing and sampling directed graphs with given degree sequences", *New J. Phys.* **14**, 023012 (2012).

**Supplementary Information** to this manuscript is provided below.

**Acknowledgments** We thank O. Barak, E. Braun, R. Meir, and M. Stern for valuable discussions and S. Marom, A. Rivkind, L. Geyrhofer and H. Keren for critical reading of the manuscript.

**Author Information** Correspondence and material requests should be addressed to N.B. (nbrenner@tx.technion.ac.il).

# Supplementary Material

## Contents

<b>1</b>	<b>Model Construction and Definitions</b>	<b>2</b>
1.1	Constructing the Network Backbone $T$ . . . . .	2
1.2	Normalizing the Initial Interaction Matrix $J_0$ . . . . .	2
1.3	Normalizing the Macroscopic Phenotype $y$ . . . . .	3
1.4	The Mismatch function $\mathcal{M}(y)$ . . . . .	4
<b>2</b>	<b>Additional Convergence Properties of Exploratory Adaptation</b>	<b>5</b>
2.1	Convergence to a Limit Cycle . . . . .	5
2.2	Dependence of Convergence in Scale-Free Networks on Pareto Distribution Parameters . . . . .	6
2.3	Convergence Dependence on Sparseness of Macroscopic Phenotype . . . . .	7
2.4	Convergence of Different Network Ensembles . . . . .	8
2.5	Stretched Exponential Fit to the Distribution of Convergence Times . . . . .	9
<b>3</b>	<b>Intrinsic Dynamics of Constant Networks</b>	<b>10</b>
3.1	Dependence of Convergence of Constant Networks on Largest Hub . . . . .	10
3.2	Dependence of Convergence of Constant Networks on Network Gain . . . . .	11

# 1 Model Construction and Definitions

## 1.1 Constructing the Network Backbone $T$

Interactions between the intracellular dynamical variables are governed by the network matrix  $W$ , a sparse matrix defined as the element wise (Hadamred) product of the backbone  $T$  and a Gaussian random matrix  $J$ :

$$W = T \circ J. \quad (5)$$

Here  $T$  is the adjacency matrix of the network with entries zero or one and  $J$  determines the strength of interactions.

An important property of the network is the distributions of its out-going and in-coming connection degrees  $P_{in}(K^{in})$  and  $P_{out}(K^{out})$ . In practice, to construct a network sampled from an ensemble with given distributions,  $T$  is constructed by first randomly sampling a list of  $N$  out-going degrees  $\{d_i^{out}\}$  from the distribution  $P_{out}(K^{out})$  with  $d_i^{out} \leq N - 1$  and then sampling a list of  $N$  in-coming degrees  $\{d_i^{in}\}$  from the distribution  $P_{in}(K^{in})$  (again  $d_i^{in} \leq N - 1$ ), conditioned on the graphically of the in and out degree sequences [2]. The network is then constructed from these sequences using the algorithm described in [1].

The scale-free sequences are obtained by a discretization to the nearest integer of the continuous Pareto distribution  $P(K) = \frac{(\gamma - 1)a^{(\gamma-1)}}{K^\gamma}$ ; Binomial sequences are drawn from a Binomial distribution  $P(K) = \mathcal{B}(N, p)$ , with  $p = \frac{\langle K \rangle}{N}$  and exponential sequences are obtained by a discretization to the nearest integer of the continuous exponential distribution  $P(k) = \frac{1}{\beta} e^{-\frac{k}{\beta}}$  with  $\beta = \langle k \rangle$ . A Binomial degree sequence is implemented using MATLAB built-in Binomial random number generator. Exponential and Scale-free sequences are implemented by a discretization of the continuous MATLAB built-in Exponential and Generalized Pareto random number generators with Generalized Pareto parameters  $k = 1/(\gamma - 1)$ ,  $\sigma = a/(\gamma - 1)$  and  $\theta = a$ .

## 1.2 Normalizing the Initial Interaction Matrix $J_0$

The initial interaction matrix  $J_0 \triangleq J(t = 0)$  is defined as a random Gaussian matrix with mean 0 and variance  $\frac{g_0^2}{\langle K \rangle}$ , where  $\langle K \rangle$  is the mean in and out degree, and  $g_0$  (the network gain) determines the spectral radius of the combined interaction matrix  $W$  at  $t = 0$ . For a uniform adjacency matrix  $T$  with average connectivity  $\langle K \rangle$  and i.i.d elements, one has  $Var(T_{i,j}) = \frac{\langle K \rangle}{N}$ , which implies  $Var(W_{i,j}) = \frac{g_0^2}{N}$ . In this case, in the thermodynamical limit  $N \rightarrow \infty$  the eigenvalues of  $W$  are uniformly distributed within a disc of size  $g_0$  in the complex plane [3, 4].

However, the distribution of the eigenvalues is affected by the finite size of the matrix and for the relevant sizes of several thousands it deviates considerably from the limiting distribution. Moreover, the adjacency matrices  $T$  which are used in our model are constructed with a specified degree sequences and therefore their elements are not i.i.d. This further affects the distribution of eigenvalues in the plane. Empirically we find that for matrices of relevant size the spectral radius of  $W$  is not greatly effected and it remains  $\sim g_0$  following the normalization  $Var(J_{0ij}) = \frac{g_0^2}{\langle K \rangle}$ , but the distribution is highly non-uniform (Fig. S1).

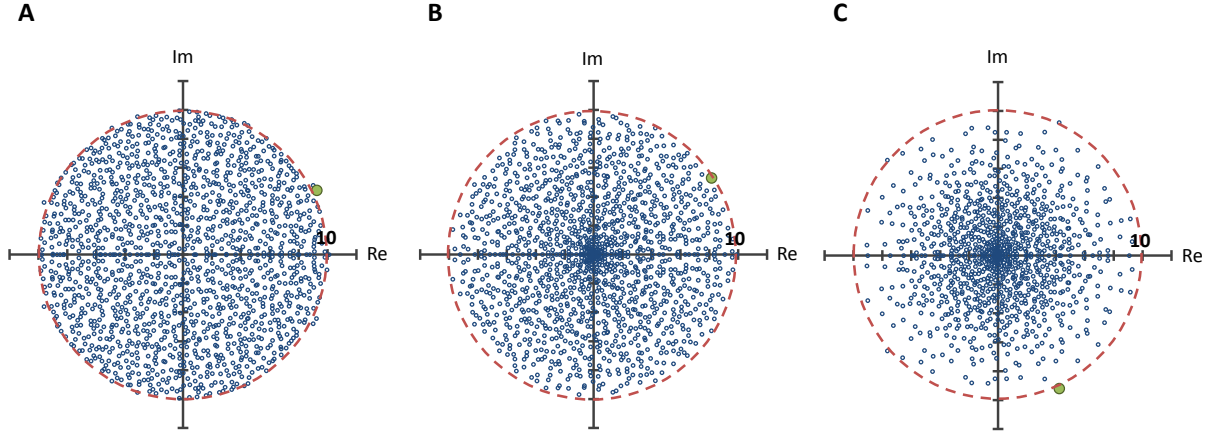


**Figure S1. Eigenvalues of finite size matrices with  $N=1500$ .** The eigenvalues of full Gaussian (A), sparse Gaussian (B) and scale-free/binomial (C) matrices are plotted. The eigenvalues of all three matrices are almost entirely contained within a disc of radius  $g_0$  (broken red) and all three have a largest eigenvalue with absolute value with norm  $\sim g_0$  (green dot). However, the distribution of eigenvalues in the disc differs considerably between the three matrices. The non-zero elements of the sparse Gaussian matrix (B) are distributed with Binomial distribution in both columns and rows. The scale-free/binomial matrix (C) has a Binomial distribution of non-zero elements in the rows and a scale-free distribution in the columns. All matrices have the form  $W = T \circ J$ , with  $J_{ij} \sim \mathcal{N}(0, \frac{g_0^2}{\langle K \rangle})$  and  $g_0 = 10$ . Binomial distributions in (B) and (C) have parameters  $p \simeq \frac{5}{N}$  and scale-free distribution in (C) has parameters  $a = 1, \gamma = 2.2$ .

### 1.3 Normalizing the Macroscopic Phenotype $y$

The variable representing the macroscopic phenotype is defined as  $y(\vec{x}) = \vec{b} \cdot \vec{x}$ . The arbitrary weight vector  $\vec{b}$  is characterized by a degree of sparseness  $c$ , i.e. the fraction of nonzero components,  $\frac{1}{N} < c < 1$ ; and by the typical magnitude of those nonzero components. In order to compare between networks of different sizes and weight vectors of different sparseness, the variance of the non-zero components is scaled by their number,  $cN$  and by the matrix gain  $g_0^2$ . The non-zero components of  $\vec{b}$  are thus distributed  $b_i \sim \mathcal{N}(0, \frac{1}{g_0^2 \cdot cN} \cdot \alpha)$ , with  $\alpha$  a magnitude parameter that determines the typical size of the phenotype in different network sizes and gains. Fig. S2 (A-C) depicts distributions of the values of  $y$  for  $\alpha = 100$  with various types of

interaction matrices  $W$ . As can be seen, these distributions are similarly shaped for a broad range of network sizes (Fig S2 A) and gains,  $g_0$  (Fig S2 B), and do not change for various network topologies (Fig S2 C). These results verify that  $y$  and  $J_0$  are appropriately normalized.

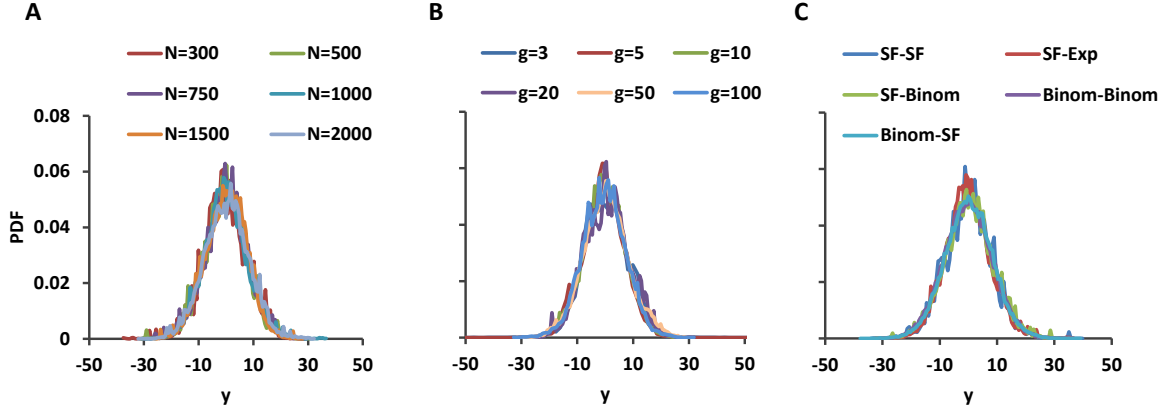


**Figure S2. Distributions of phenotype  $y$  over trajectories for various network ensembles** The distribution of the values of the macroscopic phenotype  $y = \vec{b} \cdot \vec{x}$  are plotted for various ensembles of networks with fixed interaction strengths. These include networks of various sizes (A), network gains (B) and topologies (C). For all ensembles the  $y$  values are similarly distributed. This indicates that  $y$  and  $J_0$  are appropriately normalized. For all networks  $\alpha = 100$ . Networks in (A) and (B) have Scale-free out-degree distribution and Binomial in-degree distribution; Networks in (A) and (C) have  $g = 10$  and networks in (B) and (C) have  $N = 1000$ . In all panels scale-free in/out distributions have parameters  $a = 1$  and  $\gamma = 2.4$ , exponential distributions have parameter  $\beta = 3.5$  and binomial distributions have parameters  $p = \frac{3.5}{N}$  and  $N$ .

#### 1.4 The Mismatch function $\mathcal{M}(y)$

For all computations shown in the main text, the mismatch function  $\mathcal{M}(y)$  is defined as a symmetric sigmoid

$$\mathcal{M}(y) = \frac{\mathcal{M}_0}{2} \left[ 1 - \tanh \left( \frac{|y| - \varepsilon}{\mu} \right) \right], \quad (6)$$

where  $2\varepsilon$  is the size of the low mismatch comfort zone around zero,  $\mu$  controls the steepness of the sigmoid in its dynamic range, and  $\mathcal{M}_0$  is its maximal value (see figure S3, blue line). An alternative linear mismatch function

$$\mathcal{M}(y) = \begin{cases} |x| - \varepsilon & |x| > \varepsilon \\ 0 & |x| \leq \varepsilon \end{cases} \quad (7)$$

was examined (see figure S3, red line), resulting in similar convergence properties. However, using a parabolic function for the mismatch resulted in poor convergence fractions for the same parameters displayed in the main text. Thus, the existence of a broad region of zero mismatch, rather than a well-defined minimum at a point, seems essential for convergence by exploratory adaptation, but other details of the function do not seem to have a large impact on the results.

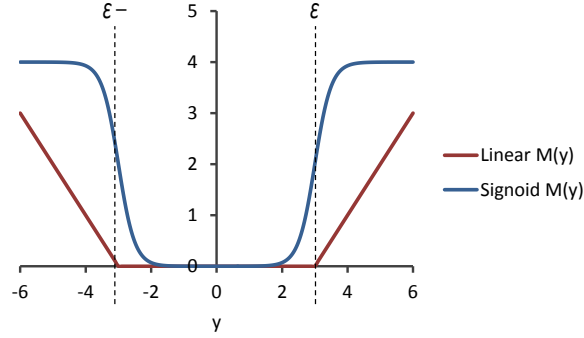


**Figure S3. Mismatch Functions** Two examples of mismatch functions  $\mathcal{M}(y)$  that result in similar convergence behavior. The results shown in the main text and supplementary were obtained using a sigmoidal mismatch function (blue); similar convergence results can be obtained with a linear mismatch function (red) as well (convergence results not shown). The sigmoidal function in the figure has parameters  $\varepsilon = 3$ ,  $mu = 0.5$  and  $\mathcal{M}_0 = 4$ .

## 2 Additional Convergence Properties of Exploratory Adaptation

### 2.1 Convergence to a Limit Cycle

An example of convergence to a fixed-point which satisfies the constraint is shown in the main text (Fig. 1 B-D). However, the non stringent constraint which is reflected in the “comfort zone” of the mismatch function  $\mathcal{M}(y)$  allows for a time-varying solutions with small amplitude which are not fixed-points. Indeed, many simulations converge to a limit cycle solution (example shown in figure S4 A, B). Such a solution satisfies the constraint only if the amplitude of macroscopic phenotype  $y$  is confined in the range  $(-\varepsilon, +\varepsilon)$  (Fig S4 A). The microscopic variables  $x_i$  also converge to limit cycles, but these can vary in amplitude and values (Fig S4 B). Interestingly for a broad range of network sizes and different network topologies the ratio between convergence of exploratory dynamics to fixed-points and to limit-cycles is largely preserved. For the ensembles shown in Fig. S4 C roughly 35% of the solutions are limit cycles and the rest are fixed-points.

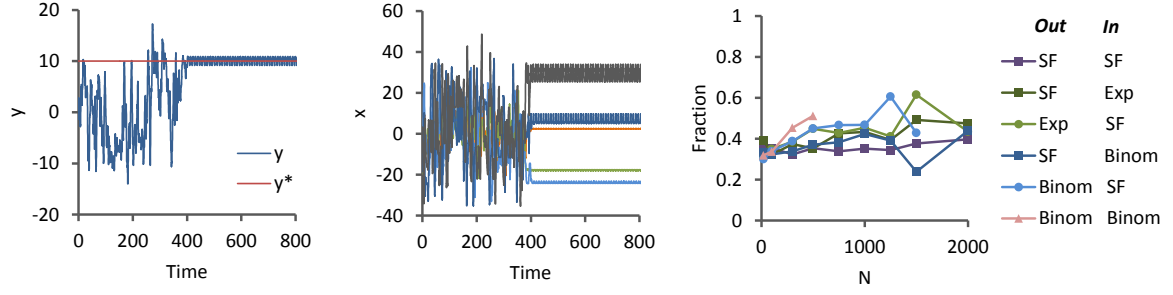


**Figure S4. Convergence to Limit Cycles.** (A) The macroscopic phenotype  $y$  as a function of time in one simulation which converged to a small-amplitude limit cycle around  $y^*$ . (B) Several microscopic variable  $x_i$  as a function of time in the same simulation which converged to a small amplitude limit cycle in  $y$ .  $x_i$  also converged to limit cycles but with various amplitudes and centers. (C) Fraction of networks that converged to limit cycles within a time window of 2000 time units, as a function of network size. Results are shown for different ensembles, each composed of a sample of 500 networks. Networks in each of the ensembles has a random  $T$ ,  $J_0$  and  $\vec{x}_0$ . The network in (A) has SF out-degree and Binomial in-degree distributions. For all networks in (A) (B) and (C)  $g_0 = 10$ ,  $\alpha = 100$ ,  $c = 0.2$   $\mathcal{M}_0 = 2$ ,  $D = 10^{-3}$  and  $\varepsilon = 3$ . In (A) and (B)  $y^* = 10$  and in (C)  $y^* = 0$ . In all panels scale-free in/out distributions have parameters  $a = 1$  and  $\gamma = 2.4$ , exponential distributions have parameter  $\beta \sim 3.5$  and Binomial distributions have parameters  $p \simeq \frac{3.5}{N}$  and  $N$ .

## 2.2 Dependence of Convergence in Scale-Free Networks on Pareto Distribution Parameters

As mentioned above, scale-free degree distributions were sampled by discretizing the continuous Pareto distribution

$$P(k) = \frac{(\gamma - 1)a^{\gamma-1}}{k^\gamma}, \quad (8)$$

where the parameter  $a$  controls the minimal value of the support and  $\gamma$  controls the power law tail of the distribution. In contrast to directly sampling from a discrete distribution such as the Zeta distribution, such a sampling method allows additional control of the lower part of the distribution. After discretization the minimal possible degree,  $k_{min}$  is the integer which is nearest to  $a$  regardless of non-integer values assigned to  $a$ . However, the exact value of  $a$  affects the weight of the distribution at its minimal value  $k_{min}$  and the overall shape of the discrete distribution at its lower part. For example, for every  $a \in [1, 1.5)$  the minimal degree in the network would be 1. However for  $a = 1.1$  there would be a higher probability for nodes with degree 1 than with  $a = 1.4$ . This allows us to examine with detail the effect of the lower part of the scale-free distribution on the convergence properties of the model. We find that the convergence of exploratory adaptation is indeed sensitive to the the weights at the lower part



of the out-going distribution (Fig. S5 A), and converges with high fractions only for networks with a large enough number of nodes with out-going degree 1 ( $a \in (0.4, 1.4)$ ). In contrast, convergence is weakly dependent on the exact power law of the distribution  $\gamma$  (Fig. S5 B).

While  $a$  and  $\gamma$  have a very different effect on the distribution, they both influence the mean degree  $\langle k \rangle$  of the network. Fig. S5 C shows the same convergence fractions plotted as a function of the mean degree. The results indicate that  $\langle k \rangle$  does not directly influence convergence fractions, and highlights the sensitivity to the lower-part of the distribution which is controlled by  $a$ . Recent findings have shown that the controllability of random networks is strongly affected by the minimal degree of the nodes with a transition when the minimal degree is increased to  $k_{min} \geq 2$  [5]. For our model we conclude that both the existence of hubs (Fig 2, 3 and S9) and the existence of a large number nodes with out-going degree 1 are indicative of convergence to a stable state.

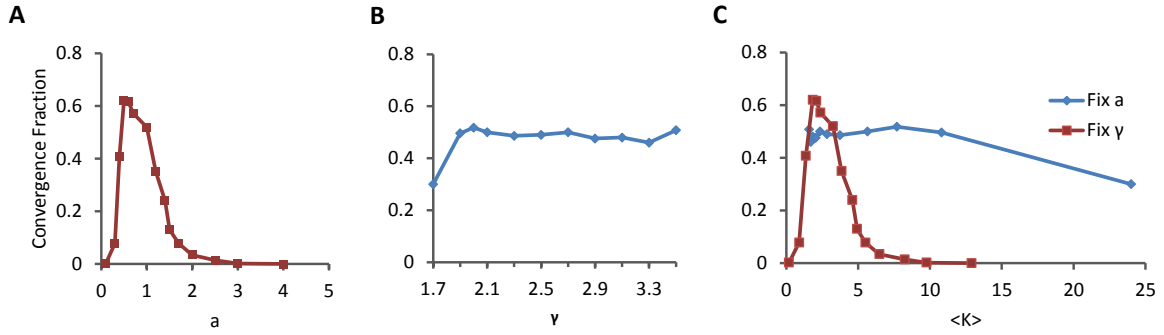


**Figure S5. Dependence of convergence fractions on parameters of out-degree Pareto Distribution.**

Scale-free degree distributions are sampled by discretizing the continuous Pareto distribution (Eq. 4). (A) Convergence fraction as a function of  $a$ , a parameter which controls the lower part of the distribution. (B) Convergence fraction as a function of  $\gamma$ , which controls the power-law tail of the distribution. (C) Convergence fraction as a function of mean degree  $\langle K \rangle$ ; changes in this mean degree can be obtained by varying  $a$  (red line) or  $\gamma$  (blue line). Each data point in (A), (B) and (C) represents the fraction of network which converged within a time window of 2000 time units from a different ensemble of 500 networks. Networks in each of the ensembles has a random  $T$ ,  $J_0$  and  $\vec{x}_0$ . All Ensembles have SF out-degree distribution and Binomial in-degree distribution. For all results  $N = 1000$ ,  $g_0 = 10$ ,  $\alpha = 100$ ,  $c = 0.2$ ,  $\mathcal{M}_0 = 2$ ,  $\varepsilon = 3$ ,  $D = 10^{-3}$  and  $y^* = 10$ . Scale-free out-degree distributions have parameters  $a = 1$ ,  $\gamma = 2.4$ , and Binomial in-degree distributions have  $p = \frac{3.5}{N}$ .

### 2.3 Convergence Dependence on Sparseness of Macroscopic Phenotype

As mentioned above the macroscopic state,  $y(\vec{x}) = \vec{b} \cdot \vec{x}$ , can have a varying degree of sparseness  $c$ . However, we find that convergence properties are not affected by changing the sparseness of macroscopic state (figure S6 A).

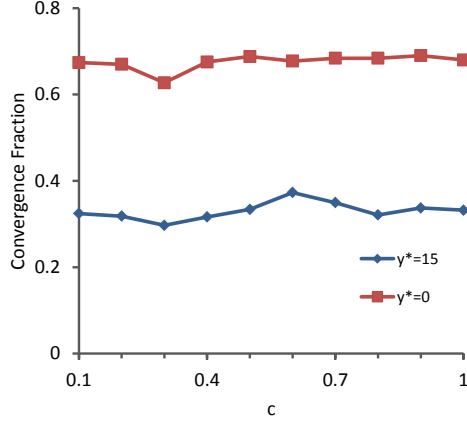


**Figure S6 Dependence of convergence fractions on the sparseness of macroscopic state vector.** Convergence properties are not affected by changing the sparseness of macroscopic state,  $c$  (A). Each data point represents the fraction of network which converged within a time window of 2000 time units from a different ensemble of 500 networks. Networks in each of the ensembles have random  $T$ ,  $J_0$  and  $\vec{x}_0$ . All Ensembles have SF out-degree distribution and Binomial in-degree distribution. For all results  $N = 1000$ ,  $g_0 = 10$ ,  $\alpha = 100$ ,  $\mathcal{M}_0 = 2$  and  $D = 10^{-3}$ ,  $\varepsilon = 3$ . SF out-degree distribution has parameters  $a = 1$ ,  $\gamma = 2.4$ , and Binomial in-degree distributions has parameters  $p \simeq \frac{3.5}{N}$  and  $N$ .

## 2.4 Convergence of Different Network Ensembles

The model we suggest includes both quenched and annealed disorder. The random topology of the network, namely the specific adjacency matrix  $T$ , is quenched and remains the same throughout the course of the simulations. The strengths of the network interactions,  $J(t)$ , on the other hand, are dynamic and change via a random walk, thus presenting an annealed disorder. When examining statistical properties of the model, one has to determine what the relevant ensemble is.

Given a choice of the model parameters, one possible ensemble  $\{(T^j, J_0^j, \vec{x}_0^j)\}_{j=1}^m$ , consists of a set of  $m$  networks, each with a different topology  $T^j$ , different initial interaction strengths  $J_0^j \triangleq J^j(t=0)$  and different initial conditions  $\vec{x}_0^j \triangleq \vec{x}^j(t=0)$ . Another potential ensemble,  $\{(T^0, J_0^j, \vec{x}_0^j)\}_{j=1}^m$ , contains of a set of networks which all share the same topology  $T^0$ , but differ in the initial network strengths  $J_0^j$ , and initial conditions  $\vec{x}_0^j$ ; A third possibility is constructing an ensemble by varying only the initial conditions  $\vec{x}_0^j$  and using the same initial network  $W^0 = T^0 \circ J_0^0$ ,  $\{(T^0, J_0^0, \vec{x}_0^j)\}_{j=1}^m$ , and finally, one can simulate the dynamics consecutively keeping both the initial network  $W^0$  and initial dynamical conditions  $\vec{x}_0^0$  constant,  $\{(T^0, J_0^0, \vec{x}_0^0)\}_{j=1}^m$ , with different realizations of the exploration process. Whether or not these various ensembles show qualitatively similar statistical properties or not is *a-priori* known and depends on the self-averaging properties of the system.

We tested these properties by computing the distribution of convergence times for the various

ensembles. Fig. S7 shows that these distributions are similarly shaped for all ensembles.

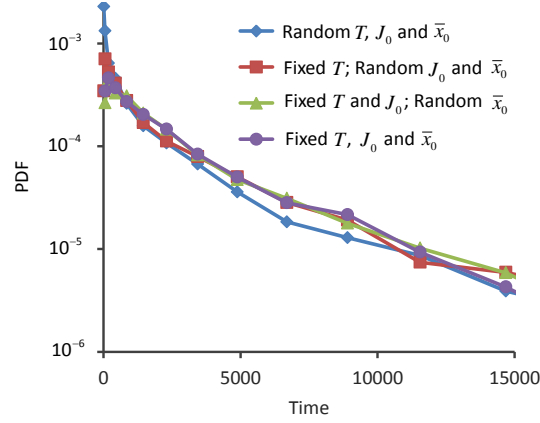


**Figure S7 Convergence Time distributions for Different Network Ensembles.** (i) An ensemble in which each network has random  $T^j$ ,  $J_0^j$  and  $\bar{x}_0^j$  (blue); (ii) An ensemble in which all networks share the same topology  $T^0$ , but differ in  $J_0^j$ , and  $\bar{x}_0^j$  (red); (iii) An ensemble in which initial network  $W = T^0 \circ J_0^0$  is the the same for all networks but initial conditions  $\bar{x}_0^j$  are unique (green) (iv) An ensemble in which both the initial network  $W^0$  and the initial dynamical conditions  $\bar{x}_0^0$  are the same for all networks. All Ensembles have SF out-degree distribution and Binomial in-degree distribution. The backbone  $T$  is the same matrix for ensembles (ii), (iii) and (iv) and the initial interactions strengths  $J_0$  is the same in ensembles (iii) and (iv). For all ensembles  $N = 1500$ ,  $g_0 = 10$ ,  $\alpha = 100$ ,  $\mathcal{M}_0 = 2$ ,  $c = 0.2$ ,  $\varepsilon = 3$ ,  $D = 10^{-3}$  and  $y^* = 0$ . SF out-degree distribution has parameters  $a = 1$ ,  $\gamma = 2.2$ , and Binomial in-degree distributions has parameters  $p = \frac{5}{N}$  and  $N$ .

## 2.5 Stretched Exponential Fit to the Distribution of Convergence Times

Convergence times of exploratory adaptation can be well fit by a stretched exponential (main text Fig 3). The fit is calculated by fitting  $1 - \log(CDF)$  of convergence times to a power law function. Thus, the fit to the CDF has the stretched exponential form  $1 - e^{-x/\lambda^k}$  which implies a Weibull distribution with PDF

$$f(t) = \begin{cases} \frac{k}{\lambda} \left(\frac{t}{\lambda}\right)^{k-1} e^{-t/\lambda^k} & x > 0 \\ 0 & x \leq 0 \end{cases} \quad (9)$$

For the distributions shown in the main text (Fig 3), the fit of  $1 - \log(CDF)$  to a power law is very good with  $R^2 \geq 0.995$ . In order to gain further understanding of the distribution of convergence times (Fig 3), we computed the empirical mean and standard divination for increasingly larger time windows. Results show that both the mean and standard divination monotonically increase with the window size (even for very large time windows - Figure S8 A and B blues). In addition

we calculated the stretched exponential fit for each time window. We did not use all the data points in each window, but rather a fixed number of 200 data points for all windows which were evenly distributed in the window. Thus we avoid the possibility of erroneous estimations of the quality of the fit stability which might result from an increase in the size of the data set for large time windows. Using this fit protocol we obtained excellent fits of  $1 - \log(CDF)$  to a power law. For all time windows above  $t=3000$  ( $R^2 \geq 0.995$ ). We also found that the fit is stable and that after an initial transient the fit parameters fluctuate very little with increased windows sizes (Figure S8 A and B reds). These findings increase our confidence in the stretched exponential fit. Moreover, although we observed an increase in mean and std with window size, they do not diverge. The stability of the fit and its large mean and std may indicate that the first two moments of the convergence times distribution may be finite but can only be estimated using much larger time windows.

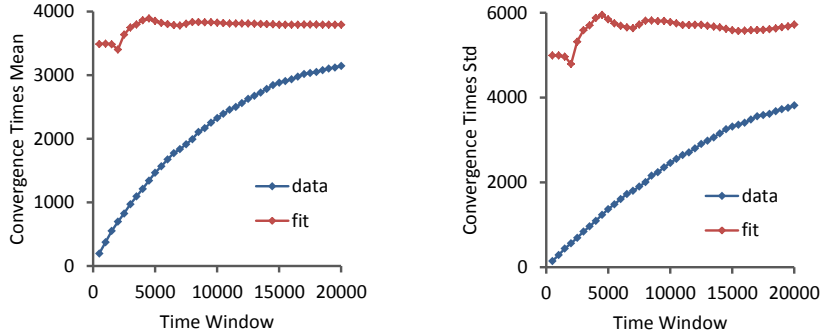


**Figure S8 Stability of stretched exponential fit to the distribution of convergence times.** the empirical mean and standard deviation for increasingly larger time windows is shown (A and B blue lines). Both monotonically increase with window size for all times tested. Mean and variance estimated from parameters of the stretched exponential fit (see text for detail) are stable and after an initial transient fluctuate very little with increased windows sizes (A and B reds). Ensemble has SF out-degree distribution with  $a = 1$ ,  $\gamma = 2.4$  and Binomial in-degree distribution with  $p = \frac{3.5}{N}$  and  $N$ . Other parameters are  $N = 1500$ ,  $g_0 = 10$ ,  $\alpha = 100$ ,  $\mathcal{M}_0 = 2$ ,  $\varepsilon = 3$ ,  $c = 0.2$ ,  $D = 10^{-3}$  and  $y^* = 0$ .

### 3 Intrinsic Dynamics of Constant Networks

#### 3.1 Dependence of Convergence of Constant Networks on Largest Hub

We have seen that convergence of exploratory adaptation depends strongly on network topology (Fig. 2 and 3 in the main text). In addition, this dependence correlates with the fraction of fixed networks (constant networks and no constraint - Fig. 4) in which the intrinsic dynamics of Eq. (1) converges to fixed points. Here we investigate further the dependence of constant networks on the network hubs. In particular, we ask whether the existence of larger hubs in a

network correlates with larger probability of convergence to fixed point. In order to examine this property we randomly constructed backbones  $T$  of size  $N=1500$  with SF out-degree and Binomial in-degree distributions. We picked 20 such backbones  $\{T_1 \dots T_{20}\}$  for which the largest hub has outgoing degrees between  $K_1 \sim 100$  and  $K_{20} \sim 1100$ . Next we created for each backbone  $T_i$  an ensembles of 500 networks, each with random interactions strengths  $\{J^{i,1} \dots J^{i,500}\}$ ,  $1 \leq i \leq 20$  (this is analogous to ensemble (ii) in fig. S7). For each ensemble we computed the fraction of networks which converged to a fixed-point in the open-loop setting. Fig. S9 depicts this fraction as a function of this largest degree, showing a noisy but significant correlation. The large fluctuation indicate that there are other properties in addition to the largest hub that have a significant influence on convergence.

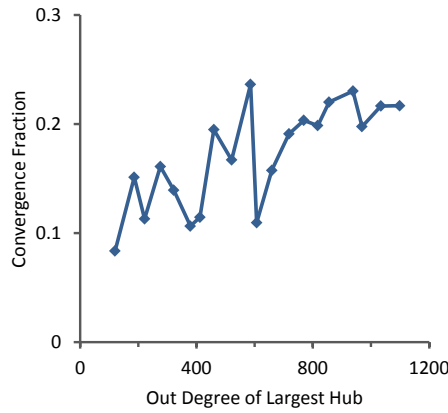


**Figure S9. Dependence of convergence fractions to fixed points in constant networks on largest hub.**

Twenty backbones  $\{T_1 \dots T_{20}\}$  were used to generate 20 ensembles, each composed of 500 random realizations of interaction strengths  $J$ . Each backbone  $T_i$  has a different maximal degree of the largest out-going hub, between  $k_1 \sim 100$  and  $k_{20} \sim 1100$ . Each data point represents the fraction of networks within the ensemble which converged to a fixed-point within a time window of 2000 in the ensemble, plotted as a function of the maximal out-degree. All backbones are drawn from a SF out-degree distribution with  $a = 1$ ,  $\gamma = 2.4$  and Binomial in-degree distribution with  $p \simeq \frac{3.5}{N}$  and  $N = 1500$  and  $g_0 = 10$ .

### 3.2 Dependence of Convergence of Constant Networks on Network Gain

Convergence fractions under exploratory adaptation dynamics are weakly dependent on the network gain  $g$  (Fig. 2 D in the main text). We examined the analogous property for constant networks by randomly constructing 5 backbones with SF out-degree and Binomial in-degree,  $\{T^1 \dots T^5\}$ . For each backbone  $T^i$  we created seven ensembles of 500 networks, each with a different  $g$ ,  $\{(T^i, J_g^j)\}_{j=1}^{500}$ ,  $1 \leq i \leq 5$ ,  $g \in \{2, 3, 6, 8, 10, 12, 15\}$  (a total of 35 ensembles). For each ensemble we computed the fraction of networks for which the intrinsic dynamics converges to a fixed-point (fixed network no constraint - Fig. S10 dotted lines). In addition we averaged over backbones by constructing seven ensembles with  $g \in \{2, 3, 6, 8, 10, 12, 15\}$  in which each

network has a different  $T$  and  $J$ ,  $\{(T^j, J_g^j)\}_{j=1}^{500}$  (Fig. S10 dark blue). Both types of ensembles show a weak dependence on  $g$  after an initial decline for small  $g$ . In addition convergence fractions are also dependent on the specific topology  $T^i$ .

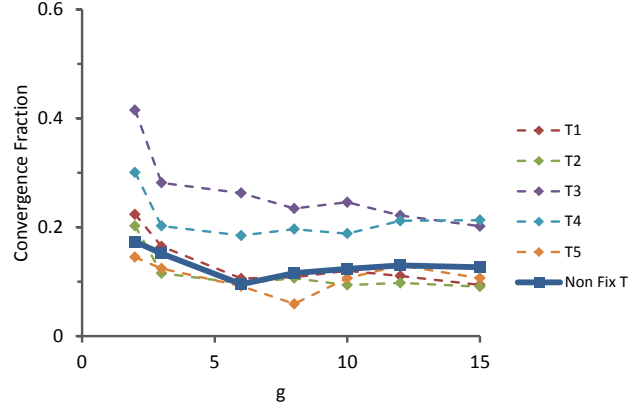


**Figure S10. Dependence of convergence fractions to fixed points in constant networks on network gain.** Ensembles of 500 networks with fixed  $T^i$ , and different  $g$ ,  $\{(T^i, J_g^j)\}_{j=1}^{500}$ ,  $1 \leq i \leq 5$ ,  $g \in \{2, 3, 6, 8, 10, 12, 15\}$  (dotted lines), were tested for converged to a fixed-point with a fixed network and no constraint. Mixing of the different backbones into ensembles characterized by  $g$  results in the thick blue line. Ensembles have SF out-degree distribution with  $a = 1$ ,  $\gamma = 2.4$  and Binomial in-degree distribution with  $p \simeq \frac{3.5}{N}$  and  $N$ ,  $N = 1500$ .

## References

- [1] H. Kim, C. I. Del Genio, K. E. Bassler, and Z. Toroczkai. Constructing and sampling directed graphs with given degree sequences. *New Journal of Physics*, 14(2):023012, 2012.
- [2] Gary Chartrand and Linda Lesniak. *Graphs & Digraphs (2Nd Ed.)*. Wadsworth Publ. Co., Belmont, CA, USA, 1986.
- [3] Crisanti A. Sompolinsky H. Sommers, H. J. and Y. Stein. Spectrum of large random asymmetric matrices. *Phys. Rev. Lett.*, 60:1895–1899, May 1988.
- [4] P.M. Wood. Universality and the circular law for sparse random matrices. *Ann. Appl. Prob.*, 22:12661300, 2012.
- [5] Giulia Menichetti, Luca Dall’Asta, and Ginestra Bianconi. Network controllability is determined by the density of low in-degree and out-degree nodes. *Phys. Rev. Lett.*, 113:078701, Aug 2014.